Xylene Isomerization over USY Zeolite in a Riser Simulator: A Comprehensive Kinetic Model

ARTICLE *in* INDUSTRIAL & ENGINEERING CHEMISTRY RESEARCH · FEBRUARY 2004

Impact Factor: 2.59 · DOI: 10.1021/ie034133f

2 AUTHORS, INCLUDING:

Sulaiman al-khattaf

King Fahd University of Petroleum and Miner…

117 PUBLICATIONS **1,120** CITATIONS

SEE PROFILE

Xylene Isomerization over USY Zeolite in a Riser Simulator: A Comprehensive Kinetic Model

A. Iliyas and S. Al-Khattaf*

Department of Chemical Engineering, King Fahd University of Petroleum & Minerals, Dhahran 31261, Saudi Arabia

The kinetics of vapor-phase isomerization of xylenes has been carried out over a USY zeolite catalyst using a fluidized-bed reactor. A comprehensive kinetic model based on the triangular reaction scheme is proposed for the reaction. The rate constants and activation energies are estimated from simplified, effective kinetic models based on the isomerization of the pure xylene isomers. The obtained results confirm an earlier proposition in the literature that the mutual interconversion of *p*- and *o*-xylenes in 1,3-methyl shifts is quite difficult as compared to intramolecular 1,2-methyl shifts. The riser simulator and associated modeling techniques are shown to be effective tools in investigating the kinetics of xylene isomerization.

Introduction

The kinetic study of catalytic isomerization of xylenes has gained considerable interest over the years. This is as a result of the significant contribution of such studies toward the understanding of the mechanism of the reaction over acid catalysts. The parameters obtained from such studies are often used in evaluating the relative magnitudes of the different reaction paths and the ease of interconversion between the three isomers. It can also be employed in designing commercial-scale reactors from experimental studies conducted in the laboratories.

In many of the available literatures, fixed-bed reactors are often utilized for the xylene isomerization reaction. However, as pointed out by Ma and Savage,[1] many difficulties are encountered in using the fixed-bed reactor for this reaction because of its complex nature. Temperature and/or concentration gradients usually occur within the flowing phase of the catalyst bed, which often affects the values of kinetic parameters reported from such studies. Differential reactors and pulsed microreactors have been applied to reduce the gradient difficulties, but analytical problems due to low conversion levels have been identified and as such minimization of the bulk phase gradient may not be assured.

It is well-known that the reaction system for xylene isomerization over zeolitic catalysts is very complicated. This is due to the presence of other side reactions, such as dealkylation, disproportionation, and transalkylation, in addition to the isomerization reaction. Several attempts have been made in the past to obtain suitable kinetic models for the reaction.[1−11] However, the complexity of the reaction and the interplay of the diffusion and chemical reactions, which causes different reaction paths, have often posed great obstacles. Consequently, two alternate reaction schemes have been proposed for the reaction in the literature. The first one, which is based on a triangular reaction path,[2−6] assumes a direct interconversion between *o*- and *p*-xylene isomers. In contrast, the second scheme assumes that the reaction proceeds via 1,2-methyl shifts following a sequence reaction path.[7−11] Furthermore, Corma and Sastre[12] and Guisnet et al.[13] have recently shown that bimolecular isomerization can contribute to the overall isomerization process for large pore zeolites. However, the dependence of this isomerization pathway on several factors such as reaction conditions, zeolite composition, and geometrical characteristics of the zeolite catalyst[12] has made its incorporation into the kinetic model very difficult.

In an earlier work, we have studied the kinetics of *m*-xylene isomerization at low conversion levels over a USY zeolite catalyst.[14] A simplified kinetic model, which excludes the disproportionation of *o*- and *p*-xylenes and the interconversion between the two isomers, was proposed. This work extends the previous study by taking into account the disproportionation of the three isomers and the possible interconversion between *p*- and *o*-xylenes in a more detailed kinetic model. A unique modeling technique, which involves the isomerization of each of the pure xylene isomers, will be employed in obtaining the numerous model parameters. In addition, the riser simulator, which is operated as a batch, well-mixed fluidized-bed reactor, will be utilized in the present study. Employing this reactor for the reaction can alleviate the problems of temperature and concentration gradients associated with fixed-bed and other reactor types. It can also ensure uniform coke deposition on the catalyst particle and ease the control of operating conditions such as temperature, time, and amount of air.

2. Experimental Section

2.1. The Riser Simulator. All of the experimental runs were carried out in the riser simulator. This reactor is a novel bench-scale equipment with internal recycle unit invented by de Lasa[15] to overcome the technical problems of the standard microactivity test. It is fast becoming a valuable experimental tool for reaction evaluation involving model compounds[16−18] and also for testing and developing new fluidized catalytic cracking in vacuum gas oil cracking.[19,20] The riser simulator consists of two outer shells, the lower section and the upper section, which allow one to load or to unload the

* To whom correspondence should be addressed. Tel.: +966-3-8601429. Fax: +966-3-8604234. E-mail: skhattaf@kfupm.edu.sa.

10.1021/ie034133f CCC: $27.50
Published on Web 02/20/2004

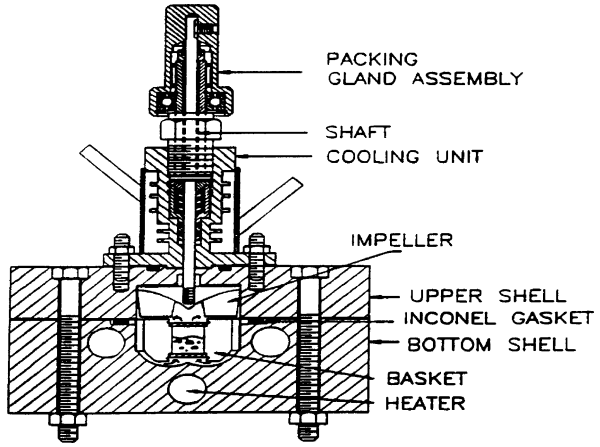

Figure 1. Schematic diagram of the riser simulator.

Table 1. Properties of the Catalyst Used in This Study

unit cell size (Å)	24.28
BET surface area (m^2/g)	155
crystal size (μm)	0.9
Na_2O (wt %)	negligible

catalyst easily. The reactor was designed in such a way that an annular space is created between the outer portion of the basket and the inner part of the reactor shell. A metallic gasket seals the two chambers with an impeller located in the upper section. A packing gland assembly and a cooling jacket surrounding the shaft provide support for the impeller. Upon rotation of the shaft, gas is forced outward from the center of the impeller toward the walls. This creates a lower pressure in the center region of the impeller, thus inducing flow of gas upward through the catalyst chamber from the bottom of the reactor annular region where the pressure is slightly higher. The impeller provides a fluidized bed of catalyst particles as well as intense gas mixing inside the reactor. A schematic diagram of the riser simulator is shown in Figure 1. A detailed description of various riser simulator components, the sequence of injection, and sampling can be found in work by Kraemer.[21]

2.2. Materials. The *m*-, *p*-, and *o*-xylenes used for the study were highly pure reagents (Fluka, purity >99%). Ultrastable Y zeolite (USY) was obtained from Tosoh Co. The Na zeolite was ion exchanged with NH_4NO_3 to replace the sodium cation with NH_4^+. Following this, NH_3 was removed and the H form of the zeolite was spray-dried using kaolin as the filler and silica sol as the binder. The resulting 60-μm catalyst particles had the following composition: 30 wt % zeolite, 50 wt % kaolin, and 20 wt % silica sol. The process of sodium removal was repeated for the pelletized catalyst. Following this, the catalyst was calcined for 2 h at 600 °C. Finally, the fluidizable catalyst particles (60-μm average size) were treated with 100% steam at 760 °C for 5 h. Table 1 reports the catalyst main properties following catalyst pretreatment. The unit cell size was determined by X-ray diffraction following ASTM D-3942-80. The surface area was measured using the Brunauer−Emmett−Teller (BET) method.

2.3. Procedure. Regarding the experimental procedure in the riser simulator, 0.8 g of catalyst was weighed and loaded into the riser simulator basket. The system was then sealed and tested for any pressure leaks by monitoring the pressure changes in the system. Furthermore, the reactor was heated to the desired reaction temperature. The vacuum box was also heated to around 250 °C and evacuated at around 0.5 psi to prevent any condensation of hydrocarbons inside the box. The heating of the riser simulator was conducted under continuous flow of inert gases (argon), and it usually takes a few hours until thermal equilibrium is finally attained. Meanwhile, before the initial experimental run, the catalyst was activated for 15 min at 620 °C in a stream of argon. The temperature controller was set to the desired reaction temperature, and in the same manner, the timer was adjusted to the desired reaction time. At this point the gas chromatograph is started and set to the desired conditions.

Once the reactor and the gas chromatograph have reached the desired operating conditions, the feedstock was injected directly into the reactor via a loaded syringe. After the reaction, the four-port valve immediately opens, ensuring that the reaction was terminated and the entire product stream sent online to the analytical equipment via a preheated vacuum box chamber.

2.4. Analysis. The riser simulator operates in conjunction with a series of sampling valves that allow, following a predetermined sequence, one to inject reactants and withdraw products in short periods of time. The products were analyzed in an Agilent 6890N gas chromatograph with a flame ionization detector and a capillary column INNOWAX, 60-m cross-linked methyl silicone with an internal diameter of 0.32 mm.

Scheme 1

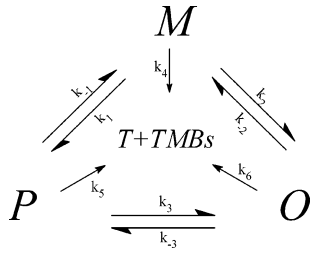

Scheme 2

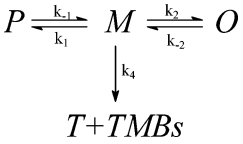

3. Kinetic Modeling

To obtain reliable and reproducible kinetic parameters, a suitable kinetic model that can adequately represent the experimental data is necessary. As a first step toward achieving this, a proper reaction scheme must be utilized. In the present study, we propose the triangular reaction scheme (Scheme 1) for the experimental data obtained based on the overall xylene isomerization process. However, this scheme involves numerous adjustable kinetic parameters, and as such it may not be feasible to estimate their values simultaneously using a single-fitting procedure. As a result, we explore the possibility of deriving simplified effective kinetic models from isomerization of *m*-xylene (Scheme 2), *p*-xylene (Scheme 3), and *o*-xylene (Scheme 4), respectively. The following assumptions are made in developing the simplified models:

Scheme 3

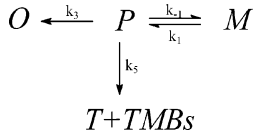

Scheme 4

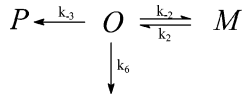

1. The isomerization and disproportionation reactions follow simple first-order kinetics.[4,7,22]

2. The reverse reactions for conversion of *p*- to *o*-xylene and *o*- to *p*-xylene are neglected in Schemes 3 and 4, respectively. This is because of the large values of C_p/C_o and C_o/C_p ratios (≈80/3) obtained from these reactions, indicating that the contribution of the reverse reaction paths in both cases can be neglected.

3. The disproportionation reaction producing toluene and trimethylbenzenes is mainly from the xylene used as the reactant.[10]

4. An irreversible reaction path is assumed for the disproportionation reaction.[7] This is substantiated by the low xylene yield (max < 3%) observed when equivalent amounts of toluene and trimethylbenzenes were reacted under different reaction conditions in this work.

5. The reactor operates under isothermal conditions,[15] which are justified by the negligible temperature change observed during the reactions.

The differential equations describing the kinetics of the xylene isomerization reaction based on the assumptions made above can be derived for each of the reacting species as follows:

m-xylene:

$$-\frac{V}{W_c}\frac{dC_m}{dt} = \varphi[(k_1 + k_2 + k_4)C_m - k_{-1}C_p - k_{-2}C_o] \quad (1)$$

$$\frac{V}{W_c}\frac{dC_p}{dt} = \varphi(k_1 C_m - k_{-1}C_p) \quad (2)$$

$$\frac{V}{W_c}\frac{dC_o}{dt} = \varphi(k_2 C_m - k_{-2}C_o) \quad (3)$$

$$\frac{V}{W_c}\frac{dC_d}{dt} = \varphi k_4 C_m \quad (4)$$

p-xylene:

$$-\frac{V}{W_c}\frac{dC_p}{dt} = \varphi[(k_{-1} + k_3 + k_5)C_p - k_1 C_m] \quad (5)$$

$$\frac{V}{W_c}\frac{dC_m}{dt} = \varphi(k_{-1}C_p - k_1 C_m) \quad (6)$$

$$\frac{V}{W_c}\frac{dC_o}{dt} = \varphi k_3 C_p \quad (7)$$

$$\frac{V}{W_c}\frac{dC_d}{dt} = \varphi k_5 C_p \quad (8)$$

o-xylene:

$$-\frac{V}{W_c}\frac{dC_o}{dt} = \varphi[(k_{-2} + k_{-3} + k_6)C_o - k_2 C_m] \quad (9)$$

$$\frac{V}{W_c}\frac{dC_m}{dt} = \varphi(k_{-2}C_o - k_2 C_m) \quad (10)$$

$$\frac{V}{W_c}\frac{dC_p}{dt} = \varphi k_{-3} C_o \quad (11)$$

$$\frac{V}{W_c}\frac{dC_d}{dt} = \varphi k_6 C_o \quad (12)$$

Regarding the catalyst deactivation function (φ) used in the above equations, it is well-known that carbon formation in catalytic cracking is responsible for the loss in activity and must be incorporated into kinetic models for catalytic cracking. Hopper and Shigemura[2] have shown that carbon formation, which is the primary cause for catalytic deactivation in the cracking reaction, is also considered to be the cause for deactivation in the xylene isomerization reaction. In this study the same exponential function based on time on stream will be employed in obtaining the model parameters for the isomerization and disproportionation reactions because both take place on the same Brönsted acid sites.[13]

The concentration of any species *i* is related to its mass fraction as follows:

$$C_i = \frac{y_i W_{hc}}{MW_i V} \quad (13)$$

while the influence of temperature on the model parameters can be accounted for through the following Arrhenius equations:

$$k_i = k_{0,i} e^{-E_i/RT} \quad (14)$$

The kinetic parameters obtained from eq 14 may show a mutual adverse effect of one parameter estimate (parameter correlation). Centering of some variables may often be helpful to reduce parameter interaction.[25] Agarwal and Brisk[26] showed that this reparametrization reduces the correlation between preexponential factors and activation energies. Therefore, k_i constants were reparametrized by centering the temperature at an average reaction temperature of T_0.

$$k_i = k_{0,i} \exp\left[\frac{-E_i}{R}\left(\frac{1}{T} - \frac{1}{T_0}\right)\right] \quad (15)$$

An important aspect in developing a reliable kinetic model for the reacting system is its thermodynamic consistency at equilibrium. This condition can be introduced in the model by enforcing that at equilibrium conditions the net rate of each reversible reaction in Schemes 1−4 vanishes by using the following relationships:[8]

$$k_{-1} = k_1/K_{pm} \quad (16)$$

$$k_{-2} = k_2/K_{om} \quad (17)$$

where $K_{pm} = (C_p/C_m)_{eq}$ and $K_{mo} = (C_o/C_m)_{eq}$ are temperature-dependent equilibrium constants for *m*- to *p*-xylene and *m*- to *o*-xylene reactions, respectively. How-

ever, an average value can be computed for both constants because the thermodynamic equilibrium concentrations of the xylenes remain fairly constant within the temperature range of this work. The xylene equilibrium concentrations are obtained from a published work.[23]

The overall kinetic model (based on Scheme 1) can be obtained as follows:

$$\frac{dy_m}{dt} = -[(k_1 + k_2 + k_4)y_m - k_{-1}y_p - k_{-2}y_o]\frac{W_c}{V} \exp(-\alpha t) \quad (18)$$

$$\frac{dy_p}{dt} = [k_1 y_m + k_{-3}y_o - (k_{-1} + k_3 + k_5)y_p]\frac{W_c}{V}\exp(-\alpha t) \quad (19)$$

$$\frac{dy_o}{dt} = [k_2 y_m + k_3 y_p - (k_{-2} + k_{-3} + k_6)y_o]\frac{W_c}{V}\exp(-\alpha t) \quad (20)$$

$$\frac{dy_d}{dt} = [k_4 y_m + k_5 y_p + k_6 y_o]\frac{W_c}{V}\exp(-\alpha t) \quad (21)$$

Each set of equations for the simplified models (eqs 1−12) involves seven adjustable model parameters that have to be estimated before a solution is obtained. However, because the evaluation of these parameters a priori is not feasible, nonlinear regression analysis will be employed in fitting the experimental data to the model, as will be discussed in the next section.

4. Results

4.1. Experimental Data. The product distribution for the isomerization of *m*-, *p*-, and *o*-xylenes over a USY zeolite catalyst is presented in Tables 2−4, respectively. In addition, traces of benzene and tetramethylbenzenes were also observed. However, the yields of these products were consistently very low, and as a result, they were neglected in subsequent analyses. It can be seen from these tables that the yield of the various products increases steadily with both reaction time and temperature. This might suggest that the obtained product yields are below the thermodynamic equilibrium values. Also, the conversion obtained during the isomerization of *o*-xylene at 350 °C is too low (<1.5%) to be reported as kinetic data. The gas chromatographic analysis for the *m*-xylene isomerization over USY zeolite at 15 s and 450 °C is shown in Figure 2.

Furthermore, it is obvious that higher conversions are obtained for the isomerization of *p*-xylene. This indicates that, under the conditions of the present study, the USY zeolite used has a higher activity for the isomerization of *p*-xylene than that for both *m*- and *o*-xylenes. This is further elucidated from the estimated rate constants, as shown in the next section. It can also be observed that the amount of toluene and trimethylbenzenes formed from the isomerization of all the three isomers is quite high. This is expected because the USY zeolite used belongs to the class of 12MR zeolites with larger pores that can accommodate the transition-state complexes required for the disproportionation reaction.[28]

4.2. Determination of Kinetic Parameters. Model-dependent variables should have a constant error variance, and the errors should be uncorrelated and normally distributed. Thus, the various kinetic parameters in eqs 1−12 were adjusted using the weighted least-squares algorithm for nonlinear parameters. Evaluation of the kinetic constants required integration of these equations. To achieve this, a computer program in a MATLAB package was developed using the classical fourth-order Runge−Kutta method of fixed interval size. The seven model parameters in each set of equations were simultaneously adjusted, and the precisions of these parameters were evaluated. The values of the preexponential factors and activation energies obtained with their corresponding 95% confidence limits (nonlinear hypothesis) are presented in Table 5. Given the reasonable parameter correlation coefficients, it can be argued that the parameters are precisely estimated. These results are particularly relevant considering the number of parameters adjusted.

Table 2. Product Distribution at Various Reaction Conditions for *m*-Xylene Isomerization[a]

temp, K	time, s	mass fraction (%)				
		m-X	*p*-X	*o*-X	T	TMBs
623	3	98.40	0.458	0.828	0.254	0
	5	98.02	0.491	0.869	0.352	0.098
	7	97.70	0.540	0.919	0.546	0.224
	10	96.90	0.699	1.034	0.762	0.541
	11	96.75	0.739	1.061	0.822	0.610
	13	96.63	0.800	1.097	0.654	0.690
	15	96.32	0.764	1.054	1.043	0.757
673	3	97.79	0.600	0.960	0.458	0.192
	5	96.68	0.909	1.204	0.698	0.507
	7	95.55	1.179	1.456	0.993	0.822
	10	94.92	1.220	1.500	1.263	1.038
	11	94.63	1.620	1.880	1.744	1.176
	13	92.38	1.626	1.929	2.000	2.060
	15	91.49	2.110	2.300	2.030	2.080
723	3	96.08	1.072	1.356	0.873	0.616
	5	91.76	2.154	2.317	1.804	1.790
	7	89.90	2.590	2.780	2.140	2.420
	10	88.70	2.810	3.030	2.490	2.813
	11	88.72	2.918	3.010	2.597	2.549
	13	86.94	2.810	3.093	3.381	3.520
	15	86.11	3.718	3.683	3.098	3.106
773	3	90.83	2.220	2.480	2.230	2.185
	5	87.96	2.890	3.110	2.824	2.940
	7	85.8	3.489	3.668	3.320	3.648
	10	83.56	3.733	3.858	4.209	4.162
	11	82.06	3.700	3.890	4.851	4.822
	13	80.22	4.345	4.454	5.159	5.210
	15	78.35	4.480	4.622	5.860	5.906

[a] Reported experimental data are averages of at least three measurements.

Table 3. Product Distribution at Various Reaction Conditions for *p*-Xylene Isomerization[a]

temp, K	time, s	mass fraction (%)				
		m-X	*p*-X	*o*-X	T	TMBs
623	3	0.615	98.40	0.201	0.577	0.191
	5	0.684	98.00	0.227	0.618	0.296
	7	0.792	97.65	0.256	0.730	0.364
	10	0.956	96.85	0.260	1.100	0.643
	15	1.287	95.71	0.306	1.541	0.973
673	3	0.966	97.51	0.290	0.693	0.347
	5	1.180	96.20	0.360	1.368	0.697
	7	1.845	94.74	0.413	1.636	1.089
	10	2.401	91.77	0.586	2.824	2.054
	15	3.869	87.59	0.832	3.963	3.182
723	3	1.923	94.87	0.502	1.436	0.951
	5	2.548	93.02	0.595	1.975	1.501
	7	3.591	89.71	0.893	2.964	2.355
	10	4.486	86.11	1.155	4.121	3.442
	15	6.191	80.24	1.649	5.856	5.095

[a] Reported experimental data are averages of at least three measurements.

Table 4. Product Distribution at Various Reaction Conditions for *o*-Xylene Isomerization[a]

temp, K	time, s	mass fraction (%)				
		m-X	*p*-X	*o*-X	T	TMBs
673	3	0.385	0.041	98.71	0.492	0.180
	5	0.565	0.062	98.16	0.600	0.354
	7	1.734	0.220	95.80	1.065	1.090
	10	1.675	0.178	95.48	1.277	1.140
	15	2.233	0.240	93.86	1.749	1.662
723	3	1.400	0.250	96.71	0.780	0.600
	5	2.094	0.374	94.92	1.281	1.136
	7	2.619	0.473	93.02	1.831	1.726
	10	4.235	0.808	89.50	2.527	2.578
	15	5.899	1.110	85.49	3.468	3.583
773	3	2.404	0.623	94.08	1.356	1.238
	5	3.508	0.827	91.31	2.030	1.925
	7	4.848	1.277	87.69	2.853	2.824
	10	5.657	1.565	84.54	3.757	3.809
	15	7.846	2.194	78.25	5.279	5.538

[a] Reported experimental data are averages of at least three measurements.

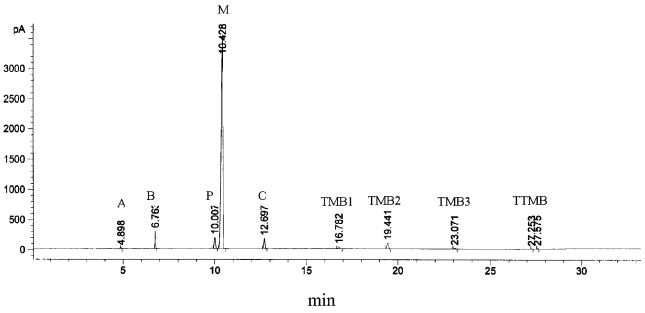

Figure 2. Gas chromatographic analysis obtained for the isomerization of *m*-xylene over USY zeolite in the riser simulator at 15 s and 723 K. A = light chain alkene, B = benzene, P = *p*-xylene, M = *m*-xylene, O = *o*-xylene, TMB1 = 1,3,5-TMB, TMB2 = 1,2,4-TMB, TMB3 = 1,2,3-TMB, TTMB = tetramethylbenzenes.

4.3. Reaction Rate Constants. From the values of the fitted kinetic parameters (Table 5), it can be seen that the order of magnitude of the reaction rate constants for the unimolecular isomerization reaction is as follows: $k_{-1} > k_{-2} > k_1 > k_2 \gg k_3 > k_{-3}$. Moreover, the rate constant for the isomerization of *p*- to *m*-xylene is initially about 3 orders of magnitude greater than that of *p*- to *o*-xylene, and it decreased by half of this value with an increase in the reaction temperature. On the other hand, the rate constant for the isomerization of *o*- to *m*-xylene is initially 140 times greater than that of *o*- to *p*-xylene and is increased to 4 times this magnitude with an increase in the temperature. Furthermore, the rate constants for the isomerization of *m*- to *p*-xylene and *m*- to *o*-xylene are closely identical, with the former being slightly higher.

It is of great interest to note that the rate constants for the disproportionation of xylenes are in the following order of magnitude: $k_5 > k_4 \approx k_6$ (Figure 3), which is consistent with the obtained experimental data. From Figure 3, it is also obvious that while k_5 varies significantly with the reaction temperature, k_4 and k_6 are less affected by temperature changes.

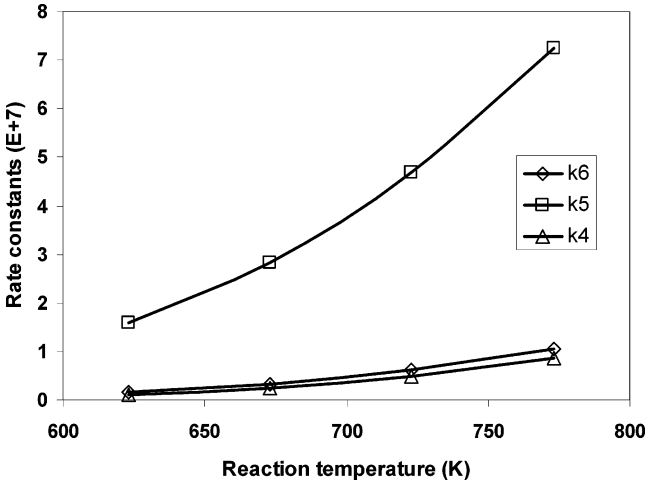

Figure 3. Xylene disproportionation rate constants vs reaction temperature.

4.4. Apparent Activation Energies. The results in Table 5 show that the apparent activation energy for interconversion of *p*- to *o*-xylene is about 6−7 kcal/mol higher than those of the other unimolecular isomerization reactions. However, it is on average about 5 kcal/mol higher than those required for disproportionation reactions. This result is in qualitative agreement with works of Hopper and co-workers[2,3] for the liquid-phase xylene isomerization over H Mordenite. Another important result is the lower value of E_5, as compared to both E_4 and E_6.

5. Discussion

5.1. Reaction Rate Constants. The observed trend in the order of magnitude of the reaction rate constants can easily be rationalized; the isomerization of xylenes on solid catalysts is considered to be an acid-catalyzed reaction, with the acidic protons of zeolites being recognized as the active sites. As a result, the extent of interaction between the acidic sites and the adsorbed species would depend on the acid strength of the sites and the basicity of the individual molecules, which is related to their dipole moment. Moreover, it has been reported in some published works that the adsorption strength of *p*-xylene is much lower than those of *o*- and *m*-xylenes.[7,30] Therefore, the faster adsorption−desorption of *p*-xylene might result in an easier intramolecular 1,2-methyl shift during the conversion of *p*-xylene compared to the other two isomers.

Table 5. Estimated Kinetics Parameters

temp, K	rate constant, k_i[a] ($\times 10^8$)								
	k_1	k_{-1}	k_2	k_{-2}	k_3	k_{-3}	k_4	k_5	k_6
623	4.06	9.02	2.75	5.96	0.008	0.004	1.14	15.91	1.59
673	7.50	16.70	5.27	11.44	0.020	0.010	2.47	28.42	3.27
723	12.75	28.37	9.24	20.00	0.050	0.030	4.83	46.87	6.08
773	20.23	45.00	15.05	32.67	0.110	0.060	8.66	72.44	10.43
E_i[b]	10.25	10.24	10.91	10.85	16.51	17.08	12.96	9.67	12.04
95% CL	1.6	1.6	1.4	1.4	0.8	1.0	0.8	1.1	1.4
$k_{0i} \times 10^3$	0.16	0.36	0.17	0.38	0.0508	0.0404	0.40	0.39	0.26
95% CL $\times 10^3$	0.042	0.042	0.044	0.044	0.034	0.023	0.08	0.068	0.04

[a] k_{0i} (m^3/kg of catalyst·s). [b] E_i (kcal/mol).

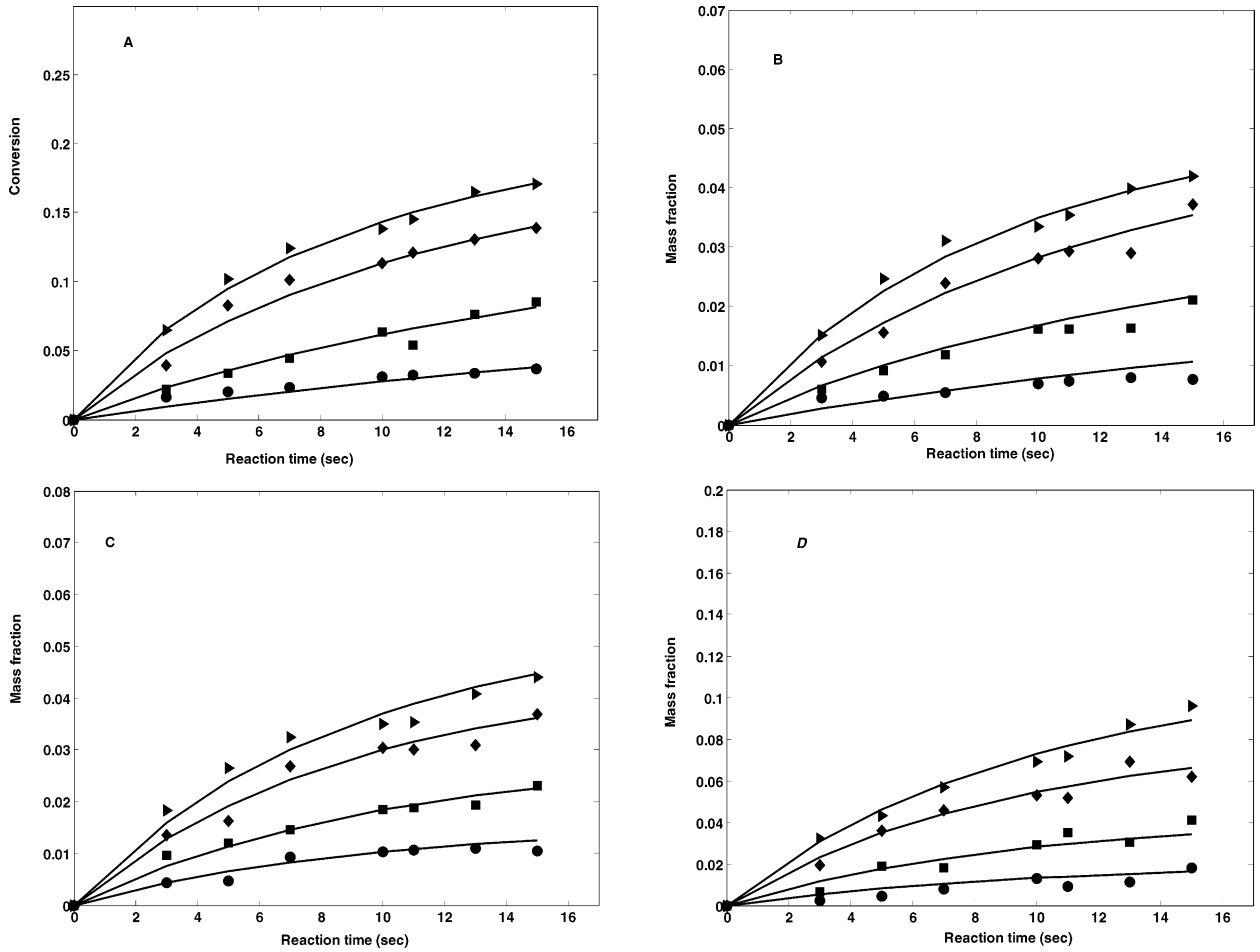

Figure 4. Comparison between experimental results and model predictions (—) based on *m*-xylene isomerization (Scheme 2): (A) *m*-xylene conversion, (B) *p*-xylene yields, (C) *o*-xylene yields, (D) T + TMBs yields. (●) 623 K; (■) 673 K; (◆) 723 K; (tilted ▲) 748 K.

On the other hand, the closely identical rate constants for the isomerization of *m*- to *p*-xylene and *m*- to *o*-xylene can be explained by the similarity of the two reactions because both involve the migration of adjacent methyl groups.[7] Moreover, this is also evident from the closeness in their estimated preexponential factors (0.16×10^{-3} and 0.17×10^{-3} (m^3/kg of catalyst·s), respectively). This is expected because the kinetic diameters of the transition-state complexes in *m*- to *p*-xylene and *m*- to *o*-xylene are lower than the cage opening of the USY zeolite used. Thus, the constraint of transition-state complexes in both reactions is negligible under the present conditions.

A very significant result is the much lower value of the estimated rate constant for the isomerization of *p*- to *o*-xylene (and vice versa) as compared to all others. This clearly indicates that the mutual interconversion between the two isomers in a 1,3-methyl migration is quite difficult, in contrast to intramolecular 1,2-methyl shifts (i.e., *m*- to *p*-xylene, *m*- to *o*-xylene, and vice versa). However, at higher reaction temperatures, this difficulty can be relatively reduced for the conversion of *p*- to *o*-xylene in comparison to *o*- to *p*-xylene conversion, as observed by the higher dependence of the former on the reaction temperature. A similar conclusion regarding the difficulty of interconversion between *p*- and *o*-xylenes based on the estimated rate constants over H Mordenite has been previously reported.[2,3] Consequently, it has been proposed that the apparent interconversion of the two isomers can only occur via

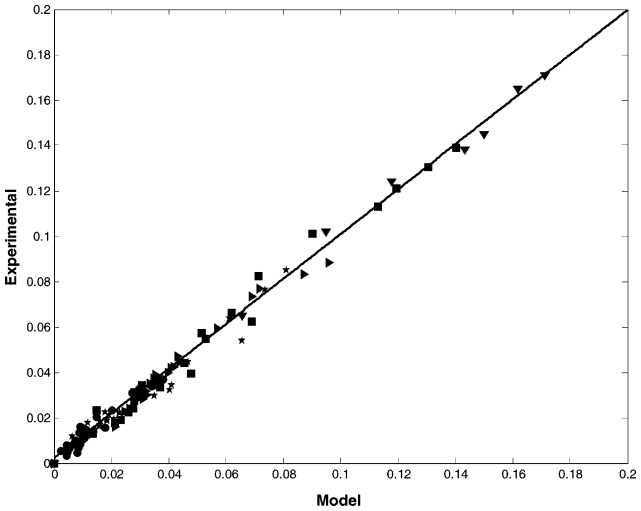

Figure 5. Overall comparison between the experimental results and model predictions based on *m*-xylene isomerization (r^2 = 0.99): (●) 623 K; (■) 673 K; (★) 723 K; (tilted ▲) 428 K.

m-xylene as an intermediate step and not directly as a single step.[9] In addition, it can also proceed via a bimolecular transalkylation reaction, with diphenylmethane as the intermediate over larger pore zeolites.[12,13,32]

Figure 3 shows that the three xylene isomers undergo disproportionation to different extents, with *p*-xylene disproportionation 10 times greater than that of *o*- and

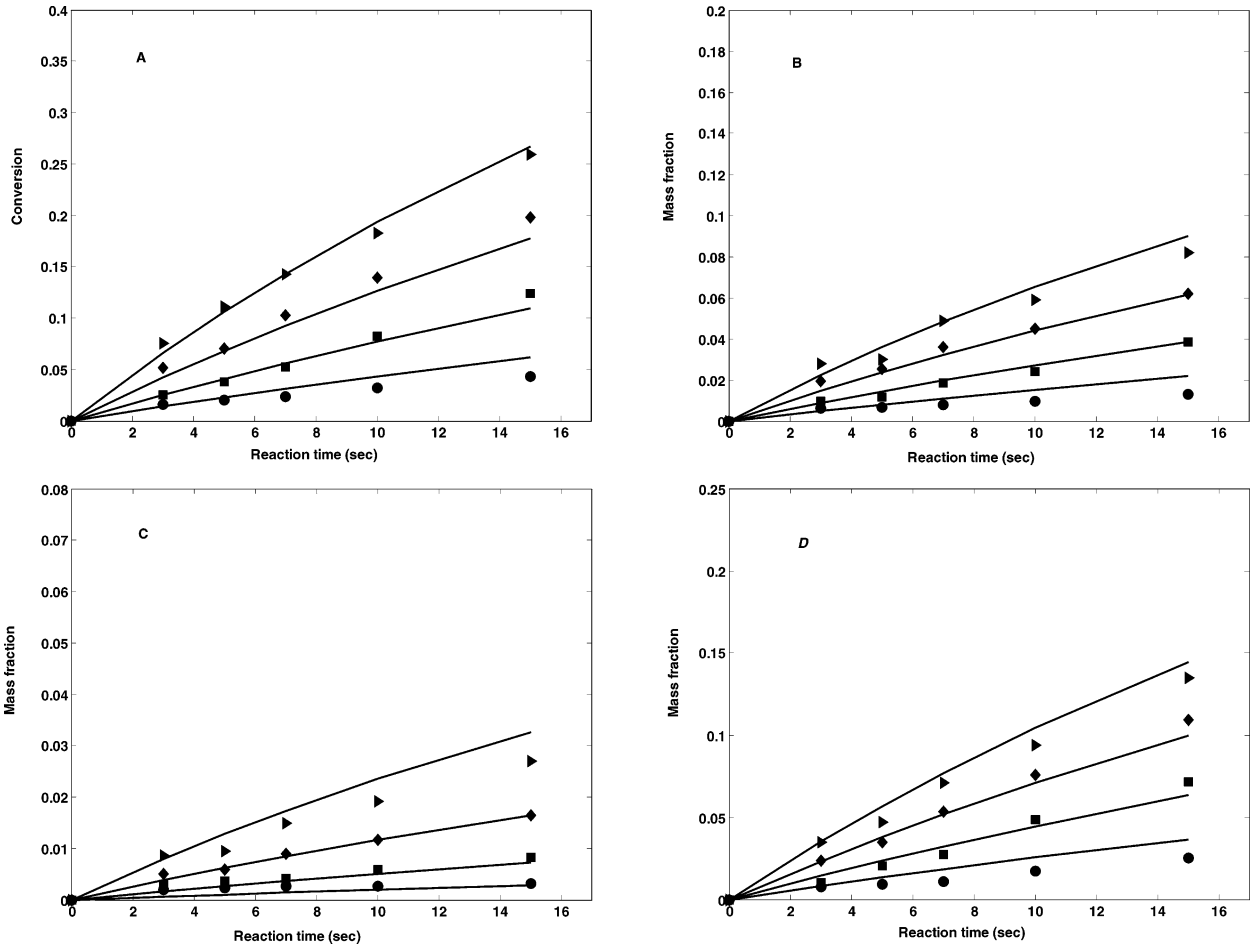

Figure 6. Comparison between experimental results and model predictions (—) based on *p*-xylene isomerization (Scheme 3): (A) *p*-xylene conversion, (B) *m*-xylene yields, (C) *o*-xylene yields, (D) T + TMBs yields. (●) 623 K; (■) 673 K; (◆) 723 K; (tilted ▲) 748 K.

m-xylene. Guisnet et al.[13] reported a similar result, with the disproportionation of *p*-xylene being 9 times faster than that of *o*-xylene. In addition, it has been shown by Lanewala and Bolton[32] that a direct correlation exits between the extent of disproportionation and conversion of the xylene isomers, with a higher disproportionation accompanying *p*-xylene isomerization. This finding, which is in perfect agreement with the results obtained in the present study, indicates that the higher reactivity of *p*-xylene is simply responsible for its corresponding greater disproportionation rate. However, Collins et al.[10] found a higher disproportionation for the less reactive *m*-xylene during xylene isomerization over HZSM5.

5.2. Activation Energies. It has been mentioned above that the mutual interconversion between *p*- and *o*-xylenes is quite difficult based on the estimated reaction rate constants for both reactions. This is further confirmed by the relatively larger values of apparent activation energies (E_3 and E_{-3}) required for the direct interconversion of the two isomers, again indicating the difficulty in causing 1,3-methyl shifts along the benzene ring.

As shown in Table 5, E_4 and E_6 are the largest, which substantiates the well-established fact that the activation energy required to move out a methyl group as a result of xylene disproportionation should be higher than that required for intramolecular methyl transfer by magnitudes of 3−4 kcal/mol.[12] However, the unexpectedly lower value of E_5 may be a result of the formation of diphenylmethane-type transition intermediates, during the disproportionation of *p*-xylene prior to further breakdown, instead of the usual carbonium ion intermediates.

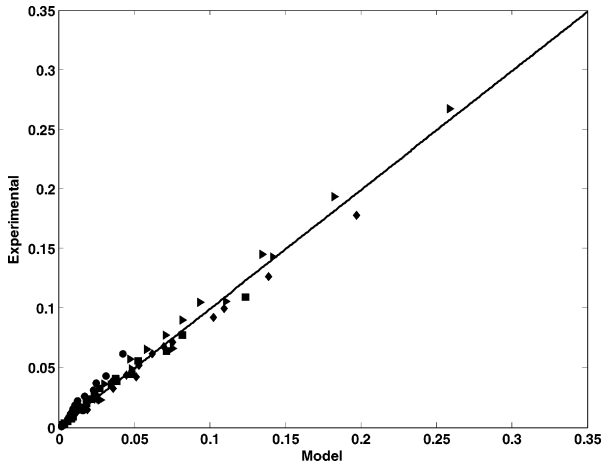

Figure 7. Overall comparison between the experimental results and model predictions based on *p*-xylene isomerization ($r^2 = 0.98$): (●) 623 K; (■) 673 K; (◆) 723 K; (tilted ▲) 748 K.

The activation energies obtained in the present work are close to those reported by Gendy[5] over a similar Y zeolite. A direct comparison with the values previously reported in the literature may not be possible considering that different catalysts were used. However, we observed that the values reported by Hsu et al.[4] and Li

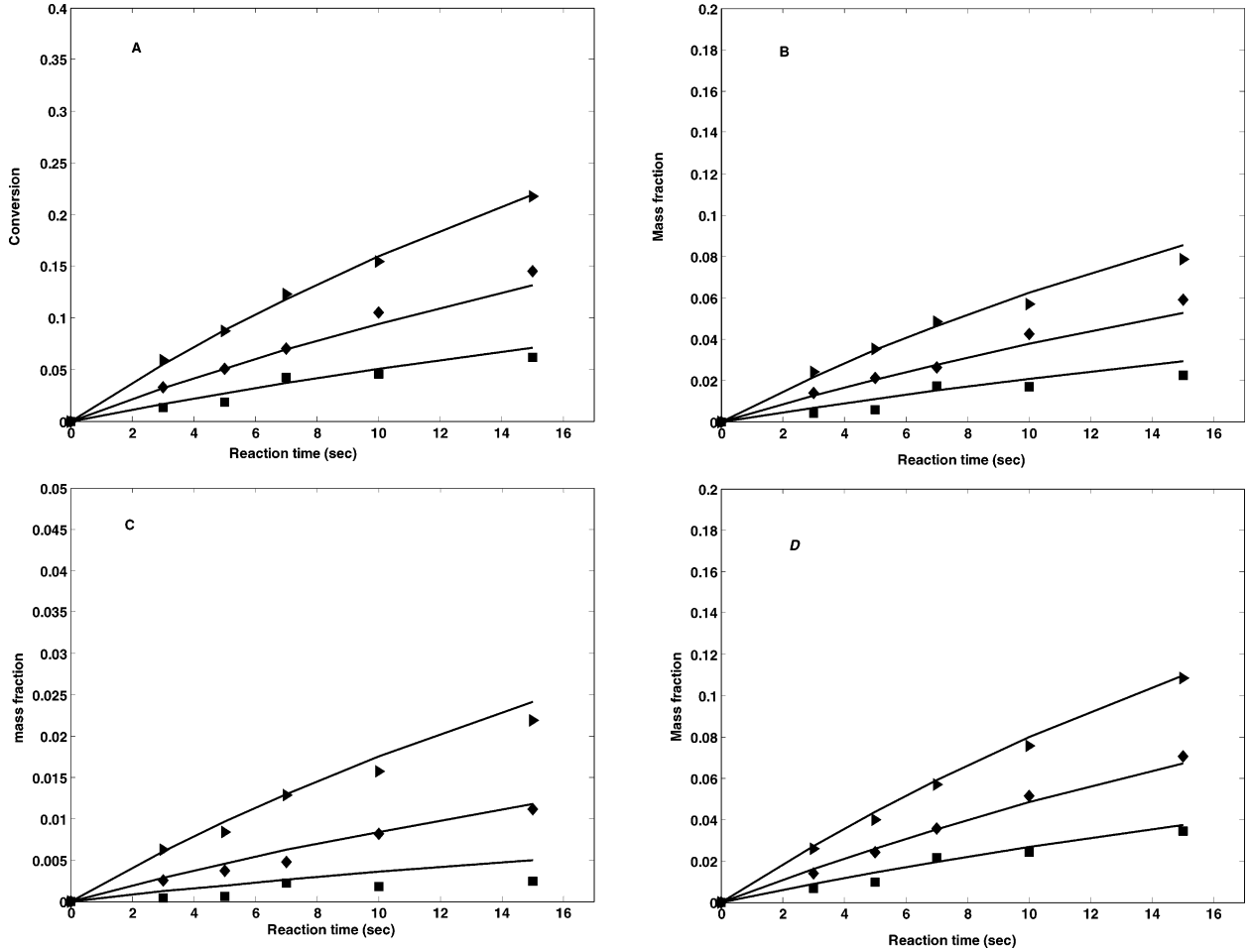

Figure 8. Comparison between experimental results and model predictions (—) based on *o*-xylene isomerization (Scheme 4): (A) *o*-xylene conversion, (B) *m*-xylene yields, (C) *p*-xylene yields, (D) T + TMBs yields. (●) 623 K; (■) 673 K; (◆) 723 K; (tilted ▲) 748 K.

et al.[30] over Pt/ZSM5 and ZSM5, respectively, are similar to those obtained in this work. On the other hand, Hanson and Engel[7] and Cappallazo et al.[5] reported substantially higher values.

5.3. Simplified Model Predictions. Figures 4−9 show the comparison between the model predictions and the experimental data at various temperatures for the simplified models. As observed in these plots, the model predictions compare favorably with the obtained experimental data for the various conditions. This provides evidence that these models could also be used for the interpretation of kinetic data following the assumptions made. In addition, the reconciliation plots (Figures 5, 7, and 9) between the experimental data and the model predictions display a normal distribution of residuals. Besides, the adequacy of the models and the selected parameters to fit the data gives 0.99, 0.98, and 0.99 regression coefficients for the isomerization of *m*-, *p*-, and *o*-xylenes, respectively.

5.4. Comprehensive Model Predictions. As mentioned earlier, the aim of this study is to develop a comprehensive model for the isomerization of *m*-xylene over USY in the riser simulator and to obtain the various model parameters. In view of this, it is indeed imperative to check the validity of the estimated kinetic parameters using with the proposed model. Moreover, the effect of reaction conditions (such as time, temperature, and catalyst life) for conditions beyond those of the present study could be simulated. Thus, the estimated rate constants were substituted into eqs 18−21,

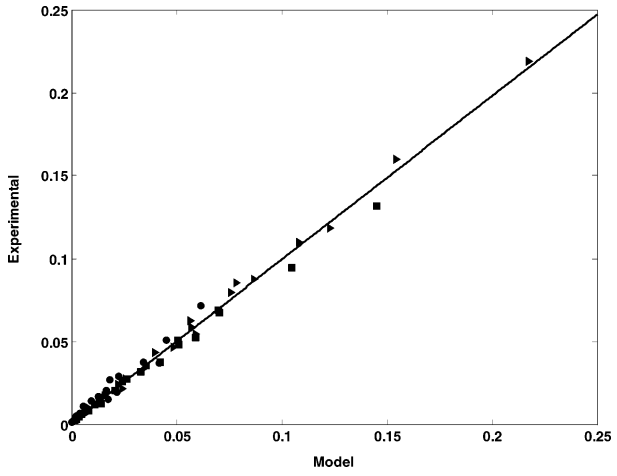

Figure 9. Overall comparison between the experimental results and model predictions based on *p*-xylene isomerization ($r^2 = 0.99$): (■) 623 K; (◆) 673 K; (tilted ▲) 773 K.

and the equations were solved numerically using the fourth-order Runge−Kutta method. The simulated results were compared with the experimental data, as shown in Figure 10. It can be observed from this figure that the simulated results compare fairly well with the experimental data, except at $T = 350$ °C, where the product yields were slightly underpredicted.

In summary, the comprehensive kinetic model proposed in the present study based on the triangular

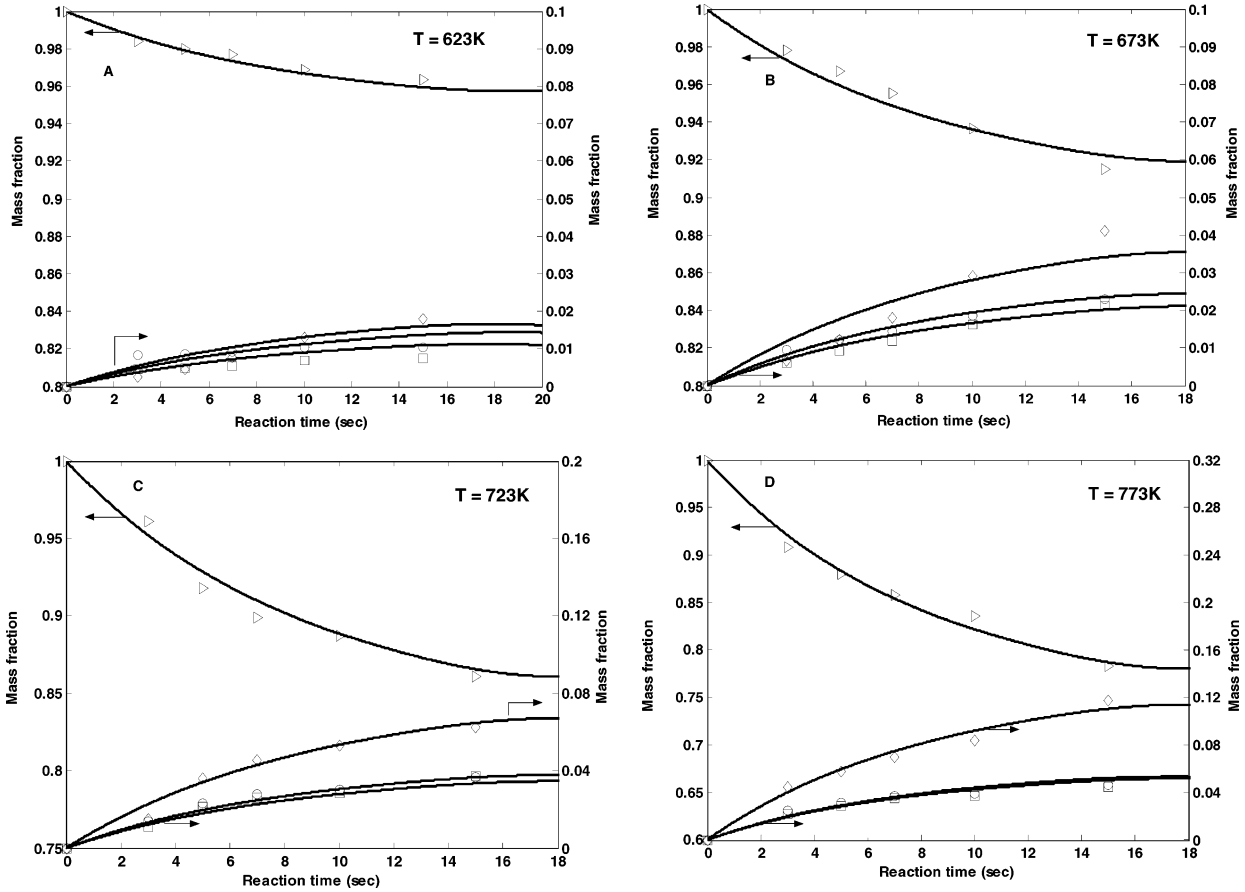

Figure 10. Comparison between experimental results and numerical solution (—) based on the overall kinetic model (Scheme 1): (A) T = 623 K: (B) T = 673 K, (C) T = 723 K, (D) T = 773 K. (tilted △) *m*-xylene conversion; (□) *p*-xylene yield; (○) *o*-xylene yield; (◇) $T+TMBS$ yield.

reaction network proved to be adequate for predicting *m*-xylene isomerization over USY in the riser simulator. However, it is worth emphasizing that the simplified models based on Schemes 2−4 are only applicable within a limited range of conversion, unlike Scheme 1, which has a wider range of application and a sounder mechanistic basis.

6. Conclusion

The kinetics of vapor-phase isomerization of xylenes has been carried out over a USY zeolite catalyst using the riser simulator. A comprehensive kinetic model that is consistent with an overall picture of the xylene reaction system based on a triangular reaction network is proposed for the reaction. Simplified effective kinetic models, which are based on the isomerization of the pure xylene isomers, are employed in obtaining the various kinetic parameters using the method of nonlinear regression analysis. The much lower values of the estimated rate constants and the relatively higher activation energies for the isomerization of *p*- to *o*-xylene (and vice versa) confirm the great difficulty for the mutual interconversion between the two isomers. Also, the higher disproportionation accompanying *p*-xylene isomerization as compared to that of *o*- and *m*-xylenes can be attributed to its corresponding higher activity over the USY catalyst used. A good comparison between the experimental data and model predictions was obtained. This provides significant evidence that the riser simulator and associated modeling technique can be used as an effective tool in the investigation of the kinetics of xylene isomerization and disproportionation reactions.

Acknowledgment

The authors gratefully acknowledge King Fahd University of Petroleum & Minerals for the financial support provided for this work under Project 255. We also thank Dr. H. I. de Lasa for his invaluable advice on the riser simulator.

Nomenclature

C_i = concentration of species i (kmol/m^3)
CFL = confidence limit
C_d = concentration of disproportionation products (T + TMBs) (kmol/m^3)
E_i = apparent activation energy for the ith reaction (kJ/mol)
K_{om} = thermodynamic equilibrium constant for the conversion of *m*- to *o*-xylene
k_i = apparent rate constant for the ith reaction (m^3/kg of catalyst·s)
$k_{0,i}$ = preexponential factor for the ith reaction (m^3/kg of catalyst·s)
K_{pm} = thermodynamic equilibrium constant for the conversion of *m*- to *p*-xylene
MW_i = molecular weight of species i (kg/kmol)
r = correlation coefficient
R = universal gas constant (kJ/kmol·K)
t = reaction time (s)

T = toluene
T_0 = average temperature of the experiment, 610 K
TMBs = trimethylbenzenes
V = riser simulator volume
W_c = catalyst mass (kg of catalyst)
W_{hc} = mass of hydrocarbon injected into the riser simulator
y_d = mass fraction of disproportionation products
φ = apparent deactivation function
α = catalyst deactivation constant

Subscripts

m = *m*-xylene
o = *o*-xylene
p = *p*-xylene
eq = equilibrium

Literature Cited

(1) Ma, Y. H.; Savage, L. A. Xylene Isomerization Using Zeolites in a Gradientless Reactor System. *AIChE J*. **1987**, *33*, 1233.

(2) Hopper, J. R.; Shigemura, D. S. Kinetics of Liquid-Phase Xylene Isomerization over H-Mordenite. *AIChE J*. **1973**, *19*, 1025.

(3) Norman, G. H.; Shigemura, D. S.; Hopper, J. R. Isomerization of Xylene over Hydrogen Mordenite. A Comprehensive Model. *Ind. Eng. Chem. Prod. Res. Dev*. **1976**, *15*, 41.

(4) Hsu, Y. S.; Lee, T. Y.; Hu, H. C. Isomerization of Ethylbenzene and *m*-Xylene on zeolites. *Ind. Eng. Chem. Res*. **1988**, *27*, 942.

(5) Gendy, T. S. Simulation of Liquid and Vapour Phase Xylene Isomerization over Deactivating H−Y Zeolite. *J. Chem. Technol. Biotechnol*. **1998**, *73*, 109.

(6) Collins, D. J.; Medina, R. J.; Davis, B. H. Xylene Isomerization by ZSM-5 Zeolite Catalyst. *Can. J. Chem. Eng*. **1983**, *61*, 29.

(7) Hanson, K. L.; Engel, A. J. Kinetics of Xylene Isomerization over Silica−Alumina Catalyst. *AIChE J*. **1967**, *13*, 260.

(8) Cappallazo, O.; Cao, G.; Messina, G.; Morbidelli, M. Kinetics of Shape-Selective Xylene Isomerization over ZSM-5 Catalyst. *Ind. Eng. Chem. Res*. **1991**, *30*, 2280.

(9) Cortes, A.; Corma, A. The Mechanism of Catalytic Isomerization of Xylenes: Kinetic and Isotopic Studies. *J. Catal*. **1978**, *51*, 338.

(10) Collins, D. J.; Mulrooney, K. J.; Medina, R. J. Xylene Isomerization and Disproportionation over Lanthaniun Y Catalyst. *J. Catal*. **1982**, *75*, 291.

(11) Sreedharan, V.; Bhatia, S. Vapour Phase Isomerization Study of *m*-Xylene over Nickel Hydrogen Mordenite Catalyst. *Chem. Eng. J*. **1987**, *36*, 101.

(12) Corma, A.; Sastre, E. Evidence of the Presence of a Bimolecular Pathway in the Isomerization of Xylene on Some Large-Pore Zeolites. *J. Catal*. **1991**, *129*, 177.

(13) Morin, S.; Gnep, N. S.; Guisnet, M. A Simple Method for Determining the Relative Significant of the Unimolecular and Bimolecular Pathways of Xylene Isomerization over HY Zeolites *J. Catal*. **1996**, *159*, 296.

(14) Iliyas, A.; Al-Khattaf, S. Submitted for publication.

(15) de Lasa, H. I. U.S. Patent 5,102,628, 1992.

(16) Al-Khattaf, S.; de Lasa, H. I. Catalytic Cracking of Cumene in a Riser Simulator: A Catalyst Activity Decay Model. *Ind. Eng. Chem. Res*. **2001**, *40*, 5398.

(17) Al-Khattaf, S.; de Lasa, H. I. Diffuision and Catalytic Cracking of 1,3,5-tri-iso-propyl-benzene in FCC Catalysts. *Chem. Eng. Sci*. **2002**, *57*, 4909.

(18) Al-Khattaf, S.; de Lasa, H. I. The Role of Difusión in Alkylbenzenes Catalytic Cracking. *Appl. Catal. A* **2002**, *226*, 139.

(19) Al-Khattaf, S. The Influence of Y-Zeolite Unit Cell Size on the Performance of FCC Catalysts During Gas Oil Catalytic Cracking. *Appl. Catal. A* **2002**, *231*, 293.

(20) Al-Khattaf, S.; de Lasa, H. I. Diffusion and Reactivity of Hydrocarbon Feedstocks in FCC Catalysts. *Can. J. Chem. Eng*. **2001**, *79*, 329.

(21) Kraemer, D. W. Ph.D. Dissertation, University of Western Ontario, London, Canada, 1991.

(22) Beschmann, K.; Riekert, L. Isomerization of Xylene and Methylation of Toluene on Zeolite HZSM5. Compound Kinetics and Selectivity. *J. Catal*. **1993**, *141*, 548.

(23) Stull, D. R.; Westrum, E. F.; Simke, G. C. *The Chemical Thermodynamics of Organic Compounds*; Wiley: New York, 1969; p 368.

(24) Bhatia, S.; Chandra, S.; Das, T. Simulation of Xylene Isomerization Catalytic Reactor. *Ind. Eng. Chem. Res*. **1998**, *28*, 1185.

(25) Draper, N.; Smith, H. *Applied Regression Analysis*, 2nd ed.; John Wiley and Sons: New York, 1981.

(26) Agarwal, A. K.; Brisk, M. L. Sequential experimental Design for Precise Parameter Estimation: 1. Use of Reparametrization. *Ind. Eng. Chem. Process Des. Dev*. 985, *24*, 203.

(27) Chirico, R. D.; Steele, W. V. Thermodynamic Equilibrium in Xylene Isomerization. *J. Chem. Eng. Data* **1997**, *42*, 784.

(28) Jones, C. W.; Zones, S. I.; Davis, M. E. *m*-Xylene Reactions over Zeolites with Unidimensional Pore Systems. *Appl. Catal. A* **1999**, *181*, 289.

(29) Martens, J. A.; Perez-Pariente, J.; Sastre, E.; Corma, A.; Jacobs, P. A. Isomerization and Disproportionation of *m*-Xylene Selectivities Induced by the Void Structure of the Zeolite Framework. *Appl. Catal*. **1988**, *45*, 85.

(30) Li, Y.; Chang, X.; Zeng, Z. Kinetics Study of the Isomerization of Xylene on HZSM-5 Zeolite. 1. Kinetics Model and Reaction Mechanism. *Ind. Eng. Chem. Res*. **1992**, *31*, 187.

(31) Mirth, G.; Cejka, J.; Lercher, A. J. Transports and Isomerization of Xylenes over HZSM-5 Zeolites. *J. Catal*. **1993**, *139*, 24.

(32) Lanewala, M. A.; Bolton, A. P. The Isomerization of the Xylenes Using Zeolites Catalysts. *J. Org. Chem*. **1969**, *34*, 3107.

(33) Ratnasamy, P.; Pokhriyal, S. K. Surface Passivation and Shape Selectivity in Xylene Isomerization over ZSM-48. *Appl. Catal*. **1989**, *55*, 265.

Received for review September 17, 2003
Revised manuscript received December 17, 2003
Accepted December 23, 2003

IE034133F